Parametric frequency tuning of phase-locked nanoelectromechanical resonators

Andreas Kraus, Artur Erbe, and Robert H. Blick[a)]
Center for NanoScience and Sektion Physik, Ludwig-Maximilians-Universität, Geschwister-Scholl-Platz 1, 80539 München, Germany

Gilberto Corso and Klaus Richter
Max-Planck-Institut für Physik komplexer Systeme, Nöthnitzer Str. 38, 01187 Dresden, Germany

(Received 25 April 2001; accepted for publication 13 August 2001)

We present measurements on nanoelectromechanical systems fabricated in semiconductor materials suited for operating frequencies in the radio band. We demonstrate how to achieve parametric frequency tuning of nanoelectromechanical resonators required for radio frequency sensor and communication applications. © *2001 American Institute of Physics.* [DOI: 10.1063/1.1412431]

One of the major applications of nanomechanical resonators is found in integrated sensor technology, requiring operating frequencies beyond 100 MHz. However, the large mechanical quality factors Q of the order of 10^4 necessary to achieve large signal-to-noise ratios, limit the range of operation to a small frequency band. In this work, we present a straightforward scheme known from optics[1] with which this limitation can easily be overcome by means of parametric frequency tuning of a phase-locked nanoelectromechanical resonator. This approach is experimentally exemplified by using rather simple nanomechanical doubly clamped beam resonators[2] and is based on well known parametric amplification as was discussed earlier for micromechanical resonators.[3]

In the present case, the nanobridges are fabricated out of silicon–metal hybrids[4] [depicted in Fig. 1(a)] as mechanical oscillators embedded in an electromagnetic circuit for demonstrating parametric frequency tuning (PFT). Important for achieving the large increase in tunable frequency range is the effective phase coupling of the nanomechanical and the electrical circuit. We observe a strong coupling of a mechanical and an electronic resonator due to internal electrical losses finally leading to PFT.

One of the samples is shown in the scanning electron microscope micrograph in Fig. 1(a) with the suspended beam magnified in the inset. The driving frequency is denoted by f, the mechanical eigenfrequency by f_0, and the pump frequency on the gate by f_p. Details of this process are discussed elsewhere.[2]

The chips are then mounted in a sample holder and a small amount of ^{4}He exchange gas is added (10 mbar) to ensure thermal coupling. We show results on two samples (A and B) placed at 4.2 K in a magnetic field. An alternating current is sent through the metallic top layer of these beams and a Lorentz force arises perpendicular to the axis of the sample and sets it into mechanical motion. For the measurements, we employ a network analyzer (HP 87511A): The output frequency is scanning the range of interest and the reflected signal is tracked. The reflected power changes when the resonance condition is met, which can be tuned by a dc gate voltage $V_g(\propto 5\ \mathrm{V})$ in a range of $\delta f_{\mathrm{dc}} \pm 2$ kHz.[2]

We investigated the response of the suspended bridges in two different geometries for the proper treatment of the clamping points causing the nonlinearity. The beam in Fig.

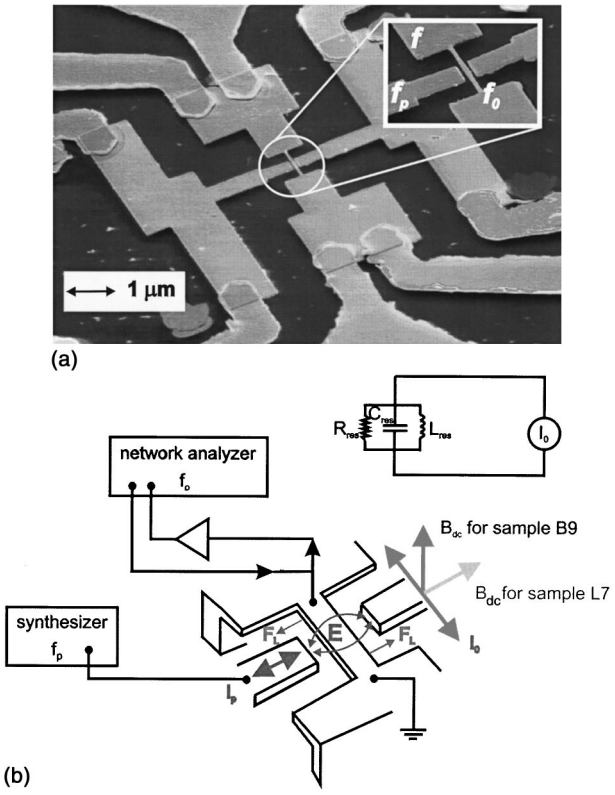

FIG. 1. (a) Scanning electron beam micrograph of one of the electromechanical resonators used (sample A). The silicon beam is covered by a thin Au sheet of 50 nm, which allows for impedance matching to the circuitry and coupling of the driving frequency f to the mechanical eigenfrequency f_0. The electrodes on the left- and right-hand side enable application of an additional dc bias and/or ac modulation at a pump frequency f_p. The effective masses of the resonators are computed to be $m^A_{\mathrm{eff}}=6.15\times10^{-16}$ kg and $m^B_{\mathrm{eff}}=9.67\times10^{-16}$ kg. The theoretically estimated resonance frequencies are of the order of $f^A_0=74$ MHz and $f^B_0=72$ MHz, while the eigenfrequencies obtained by SOLVIA are 95.93 MHz and 81.7 MHz, respectively. Inset shows a magnification of the nanobridge. (b) Experimental setup for sampling the mechanical properties of the suspended beam. Inset shows a circuit diagram with R_{res}, C_{res}, and L_{res} used to model mechanical resonators.

a)Electronic mail: robert.blick@physik.uni-muenchen.de

1(a) (sample A in this case) has a length of $l=1.82\,\mu$m, a width of $w=200$ nm, and a height of $h=250$ nm, is clamped on both ends, and the magnetic field is oriented perpendicular to the sample plane. Due to the arising Lorentz force, this translates into an in-plane displacement. The other resonator (termed B) has a slightly different geometry: $l=4.8\,\mu$m, $w=170$ nm, and $h=240$ nm, while the magnetic field is fixed in plane, leading to an out-of-plane displacement [see Fig. 1(b)]. The two nanoresonators allowed us to verify PFT for two different magnetic field configurations, by pumping with a Marconi 2032 synthesizer at a frequency $f_p \sim f_0$ on one of the side gates. This mode couples capacitively to the mechanical resonator with an estimated capacitance of $C_{\text{gate}} \sim 0.2$ fF for sample A and ~ 0.6 fF for sample B. The reflected power is finally amplified and detected by the network analyzer. The elastic properties of the suspended nanobridges were modelled by using the software tool SOLVIA[5] (in linear response).

In Figs. 2 (sample A) and 3 (sample B) the radio frequency response is depicted for different pumping frequencies at a fixed magnetic field strength. The excitation power of the network analyzer was fixed at -50 dBm. The mechanical quality factor, $Q=f/\delta f$, of the resonators under test in the linear regime are $Q^A=1.37\times10^3$ and $Q^B=2.73\times10^3$. The fundamental resonance frequency is given by $f_0=\omega_0/2\pi\cong(E/\rho)^{1/2}d/l^2$ where E is Young's modulus, ρ is the material density, and d is the beam's thickness—for Au $E=8.0\times10^{10}$ N/m^2, $\rho=19.32\times10^3$ kg/m^3, and for Si$E_{(100)}=1.7\times10^{11}$ N/m^2, $\rho=2330$ kg/m^3.

As seen in Fig. 2(a), the profile of most of the resonance curves follows a Lorentzian shape corresponding to the linear response regime. For the other resonator discussed next, we find the transition from a symmetric resonance shape to an asymmetric, sawtooth shape, characteristic of an oscillator operated in the nonlinear regime (Fig. 3).[2,6] The resonance maximum shifts by $\delta f_{\text{ac}}=130$ kHz or vanishes at all for $f_p=f_0=95.90$ MHz [Fig. 2(a)]. A more complete view is given in Fig. 2(b): The resonance structure is shown in grayscale representation where dark regions correspond to energy absorption by the beam, i.e., a mechanical resonance, while the bright regions indicate zero displacement. The plot is spanned by the frequencies f and f_p. Direct cross talk is seen in the intersectioning line with linear slope. The mechanical resonance is found around 95.9 MHz and is strongly distorted when the pumping frequency approaches 95.7 MHz. The mechanical oscillator then locks to $f_p=f_0=95.77$ MHz, where the shift of the eigenfrequency is of the order of 130 kHz. The power level of the driving signal at frequency f is found to be relatively low at $P=-63$ dBm, while a large field strength is required for the pumping signal at f_p with $P_p=+2$ dBm.

In conventional measurements, a frequency shift corresponding to an effective tunable frequency range of $\delta f_{\text{dc}}\cong\pm2$ kHz under $V_{\text{dc}}=\pm3$ V is found.[2] The large frequency shift of $\delta f_{\text{ac}}\cong\pm130$ kHz is only possible since the mechanical properties of the beam are modified under the action of a radio frequency signal in resonance with the mechanical circuit (denoted as maximum amplitude). A further increase of f_p leads to a complete localization of the levers, marked by minimum amplitude. In between these two, the frequency

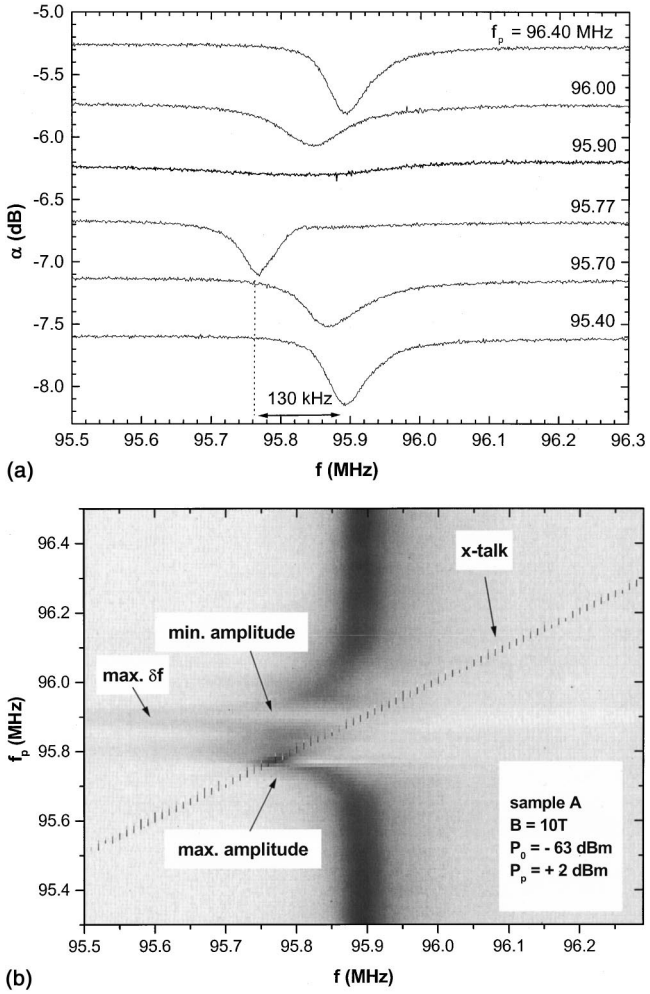

FIG. 2. (a) Typical response of a nanomechanical resonator around 95 MHz (sample A) with different pumping frequencies f_p applied as noted. The Lorentzian resonance shape indicates the linear response of the resonator. The ac frequency leads to a shift of the resonance frequency of $\delta f_{\text{ac}}=130$ kHz, compared to $\delta f_{\text{dc}}=4$ kHz for a dc bias on the gate electrode (Ref. 2). Note the complete attenuation of the resonance at $f_p=95.90$ MHz, corresponding to dynamic localization of the resonator oscillation. (b) Complete spectrum of the data from (a) shown in a gray scale plot: The dark regions correspond to the mechanical resonance. The cross talk of the pumping frequency is seen in the dashed diagonal line.

shift δf has its maximum. This corresponds to a softening of the mechanical resonance mode, i.e., the restoring force is changed under the action of a dynamic excitation. Such a behavior is characteristic for frequency tunable parametric resonators. The parametric excitation obviously allows us to increase the tunable frequency range by two orders of magnitude.

We also realized PFT in the slightly larger device (sample B): The resonator is excited well into the nonlinear regime as indicated by the resonance shape (see Fig. 3). The tunable frequency range in this case is approaching $\delta f \sim 400$ kHz and is even larger compared to sample A, while the applied field strengths are of the same order of magnitude. Clearly, this larger tunable frequency range is due to the increase in length, while the sign changes results from the different elastic moduli of Au and Si and, hence, the constants describing the nonlinearity [see Eq. (1) next] when the bridge is moving perpendicular to the sample plane. The increased noise in the tuning regime results from the direct

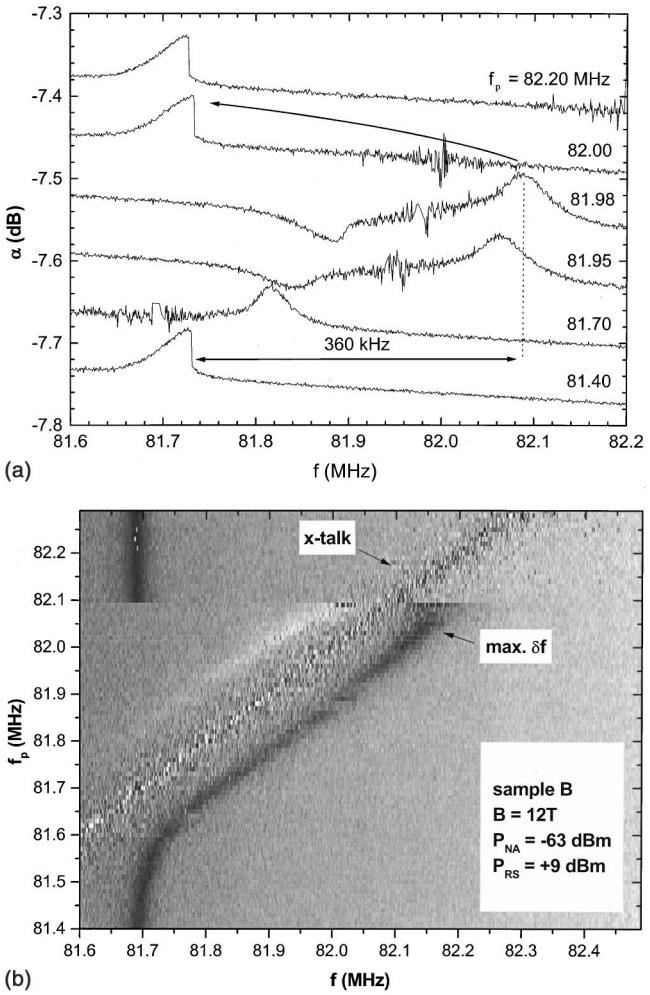

FIG. 3. Line plots (a) and gray scale plot (b) of parametric resonance tuning of sample B. The resonator is operated in the nonlinear regime, indicated by the resonance shape. In contrast to sample A, the frequency shift δf_{ac} is positive due to the different mechanical properties of this beam.

cross talk of the pumping frequency and can be eliminated by properly filtering the response. In order to achieve maximal frequency shift, it is necessary to apply a large excitation power of the driving as well as the pumping signal. The sign of the frequency shift can be adjusted by selecting the proper mechanical mode, e.g., an in-plane displacement of the beam in the fundamental mode usually leads to a negative shift of the resonance frequency.

The force $F(t)$ acting on the nanoresonator due to the radio frequency current in the capacitor is given by $F=qE$, where $E=E_0e^{i\omega_p t}$ is the electric pumping field and $q=\int I dt$, with $I=I_0\exp[i(\omega t+\phi)]$ the current running through the bridge. The phase ϕ is a free parameter of the system and the frequency is defined as usual as $\omega=2\pi f$. We obtain $F\propto\exp[i((\omega+\omega_p)t+\phi)]$ for our experimental situation $\omega_0\approx\omega\approx\omega_p$, hence, the signal at the capacitor is roughly twice the eigenfrequency ω_0 of the nanoresonator, which leads to the parametric resonance depending on the value of ϕ. In the experimental situation, we vary $\omega_p=2\pi f_p$, while keeping the other parameters constant. As noted before, we find that when ω_p is approaching ω, the two oscillations are synchronized, i.e., $\phi=$const. To explain the synchronization, we should first take into account the existence of damping caused by eddy currents.[7] Additionally, coupled nonlinear oscillations tend to synchronize when a damping mechanism is introduced.[8] Furthermore, minimal coupling energy demands the condition $\phi=0$, which implies that the nanoresonator is functioning as a parametric resonator. With all these ingredients, we can write the equation of motion for the nanoresonator as

$$\ddot{y}(t)+\mu\dot{y}(t)+\omega_0^2[1+\epsilon\cos[(\omega+\omega_p)t+\phi]]y(t)+k_3y^3(t)+k_5y^5(t)=F(t), \quad (1)$$

where $F(t)$ is the Lorentz force due to the constant external magnetic field B and $y(t)$ the displacement of the beam, while ϵ defines a coupling constant. For sample A, following Ref. 7, we have $F(t)=I_0lB/m_{\text{eff}}\cos(\omega t)$. For sample B, we have a similar $F(t)$, although the direction of the magnetic field is orthogonal (as compared to sample A). The prefactor k_3 of the cubic term in Eq. (1) determines to leading order the strength of the nonlinearity. For the two samples discussed here, we find $k_3^A=-1.81\times10^{32}\,(\text{ms})^{-2}$ and $k_3^B=+5.85\times10^{29}\,(\text{ms})^{-2}$. We note that from these constants, the frequency shift for sample A follows while for sample B effects of higher nonlinearities have to be included (k_5). Detailed calculations are shown elsewhere.[6]

In summary, we presented measurements demonstrating the application of a nanomechanical resonator for parametric frequency tuning at frequencies up to 100 MHz. This results in an increase in tunable frequency range by two orders of magnitude, finally overcoming the most severe limitation of nanoelectromechanical systems. Since nanoelectromechanical devices can be excited purely by capacitive driving, we foresee a broad variety of applications in the field of scanning probe microscopy, sensor, and communication technology. Moreover, it has to be pointed out that the phase coupling enables such a nanomechanical resonator to be applied for radio frequency circuit clocking. A very promising experiment will be the combination of PFT and quantum noise squeezing for quantum nondemolition measurements in nanomechanical systems.[9]

The authors would like to thank J.P. Kotthaus for discussion and A. Kriele and S.M. Manus for expert technical help. They acknowledge financial support by the Deutsche Forschungsgemeinschaft (DFG) via project B1-487/1.

[1] D. Magde and H. Mahr, Phys. Rev. Lett. **18**, 905 (1967).
[2] H. Krömmer, A. Erbe, A. Tilke, S. M. Manus, and R. H. Blick, Europhys. Lett. **50**, 101 (2000); D. W. Carr, S. Evoy, L. Sekaric, H. G. Craighead, and J. M. Parpia, Appl. Phys. Lett. **75**, 920 (1999).
[3] D. Rugar and P. Grütter, Phys. Rev. Lett. **67**, 699 (1991); K. L. Turner, S. A. Miller, P. G. Hartwell, N. C. MacDonald, S. H. Strogatz, and S. G. Adams, Nature (London) **396**, 149 (1998); D. W. Carr, S. Evoy, L. Sekaric, H. G. Craighead, and J. M. Parpia, Appl. Phys. Lett. **77**, 1545 (2000).
[4] A. N. Cleland and M. L. Roukes, Appl. Phys. Lett. **69**, 2653 (1996); L. Pescini, A. Tilke, R. H. Blick, H. Lorenz, J. P. Kotthaus, W. Eberhardt, and D. Kern, Nanotechnology **10**, 418 (1999).
[5] SOLVIA, version 1.1, (1997).
[6] A. Erbe, G. Corso, H. Krömmer, A. Kraus, K. Richter, and R. H. Blick, Appl. Phys. Lett. **77**, 3102 (2000).
[7] A. N. Cleland and M. L. Roukes, Sens. Actuators A **72**, 256 (1999).
[8] D. V. Ramana Reddy, A. Sen, and G. L. Johnston, Phys. Rev. Lett. **80**, 5109 (1998).
[9] M. F. Bocko and R. Onofrio, Rev. Mod. Phys. **68**, 755 (1996).